

Polymerised bicontinuous microemulsions as stationary phases for capillary electrochromatography

Effect of pore size on chromatographic performance

Kelly J. Flook^a, Neil R. Cameron^{a,*}, Stephen A.C. Wren^b

^a Department of Chemistry, University of Durham, South Road, Durham DH1 3LE, UK

^b AstraZeneca, Silk Business Park, Macclesfield, Cheshire SK10 2NA, UK

Available online 26 June 2004

Abstract

Monolithic columns for capillary electrochromatography (CEC) were prepared by in situ polymerisation of bicontinuous microemulsions containing butyl methacrylate. The resulting monoliths were found to be permeable to mobile phase flow and their behaviour as CEC stationary phases was investigated. It was found that the monoliths were able to separate a simple test mixture of phthalates, but that efficiencies were low. However, several advantages of the monoliths compared to conventional ODS packed columns were found: preparation time is short, many columns can be prepared from the same batch of microemulsion and column conditioning is much faster. The columns show promise as stationary phases for CEC, but more development is required to improve efficiencies.

© 2004 Elsevier B.V. All rights reserved.

Keywords: Electrochromatography; Stationary phases, electrochromatography; Monolithic columns; Pore size; Thermodynamic parameters

1. Introduction

Capillary electrochromatography (CEC) is an analytical separation technique that employs the separation principles of HPLC and the electroosmotically-driven mobile phase flow of capillary electrophoresis [1–3]. It has been in development for several years and stationary phase materials have been produced for a diverse range of applications. However, the limitations of capillaries packed with bead-type conventional chromatographic packing materials has led to the development of stationary phases prepared in situ in the form of hydrogels or solid porous monoliths, for which there is a wide range of preparation methods.

Columns for CEC have been developed using a variety of procedures to eliminate the need for frit fabrication, one of the major limitations of particulate packings. Monolithic columns, where the bed is microfabricated in an inorganic material [4], is one option. Several methods have been employed using modified silica beads to produce continuous beds [3,5–10]. Sintered octadecylsilica columns have been

prepared from traditionally packed CEC columns; the retaining frit was removed to eliminate the inhomogeneities [5]. ODS-modified silica gels [9] and silica particles embedded in a sol–gel column [11] have been used for the separation of enantiomers (amino acids).

Hydrophobic hydrogels prepared from acrylamides [6] have been used for the separation of polyaromatic hydrocarbons and steroids. Monoliths obtained from water soluble monomers [12–14] have also been employed. Solid monoliths have been prepared from butyl methacrylate and ethylene dimethacrylate and studied extensively, for the separation of basic pharmaceuticals [15], polycyclic aromatic hydrocarbons [16] and benzene derivatives [17–19]. Poly(styrene–divinylbenzene) supports have also proven suitable for CEC [20,21]. Enantiomeric separations have also been performed with monolithic columns [22–26] and a monolithic chiral ligand-exchange phase has been used for the chiral separation of underivatized amino acids [27]. Josic et al. have reviewed the use of monoliths for the separation of proteins and polynucleotides [28]. The analysis of plant extracts has been successfully transferred from HPLC to CEC using monolithic macroporous polyacrylamide columns [29].

* Corresponding author. Fax: +44 191 3844737.

E-mail address: n.r.cameron@durham.ac.uk (N.R. Cameron).

Previously we described the potential use of polymerised bicontinuous microemulsions as stationary phases for capillary electrochromatography. An extensive investigation of the preparation of porous materials by the microemulsion route was undertaken [30] and conditions were identified that allowed the formation of homogeneous monoliths inside capillaries through which mobile phase solutions could permeate. We now report on the effect of monolith pore size and operating parameters on chromatographic performance, for an initial sub-set of the materials investigated.

2. Experimental

2.1. Chemicals, materials and instrumentation

The monomers butyl methacrylate (BMA) and ethylene dimethacrylate (EDMA) were purchased from Sigma–Aldrich and the inhibitors were removed by passing through a short pad of basic alumina. α, α' -Azobisisobutyronitrile (AIBN) was purchased from BDH (Poole, UK). Methanol and ethanol were supplied by Fischer. Phosphoric acid (85%), dipropyl phthalate, diphenyl phthalate and thiourea were gifts from Astra Zeneca (Macclesfield, UK). All other components were purchased from Sigma–Aldrich; 1-propanol (99%), sodium dodecyl sulfate (SDS) (97%). Acetonitrile was of HPLC grade and supplied by BDH. Packed CEC capillaries (Hypersil C₁₈ CEC) were supplied by ThermoHypersil (Runcorn, Cheshire). Fused silica capillaries were supplied by Composite Metals (Worcs., UK).

2.2. Preparation of capillary columns

The parent microemulsions used for the monolithic supports were prepared by mixing components as detailed in our previous communication [31]. Microemulsion compositions can be found in Table 1. In each case, an optically clear microemulsion formed easily on agitation. Prior to polymerisation, the microemulsions were purged with nitrogen for 10 min in a sealed glass vial. This microemulsion was

Table 2
Buffers used in CEC tests

	Phosphate buffer		Water	Acetonitrile	
	Amount (μ l)	Concentration (mM)	Amount (ml)	Amount (ml)	%
1	100	0.5	1.90	8.0	80
2	100	0.5	2.90	7.0	70
3	100	0.5	3.90	6.0	60
4	100	0.5	4.90	5.0	50
5	100	0.5	5.90	4.0	40
6	50	0.25	4.95	5.0	50
7	200	1.0	4.80	5.0	50
8	300	1.5	4.70	5.0	50
9	400	2.0	4.60	5.0	50
10	500	2.5	4.50	5.0	50
11	600	3.0	4.40	5.0	50

then filled into 100 μ m i.d. capillaries to 30 cm of a 50 cm length of capillary. After sealing the ends, the capillaries were placed in an oven at 60 °C for 20 h. The unused microemulsion was polymerised alongside the capillaries, in order to characterise the monolith morphology without destroying the capillary. The polyamide coating was removed from the capillary close to the packing by electrical heating to produce a detection window required for on-line detection. It was determined that a low heater setting for a longer period prevented damage to the capillary packing enabling the dead volume between the stationary phase and the window to be reduced. Columns were inspected carefully with an optical microscope for defects in the packing material before use in CEC.

2.3. Chromatography

CEC experiments were carried out using a Beckman Coulter P/ACE MDQ Methods Development System with detection by UV detection at 214 nm. The column temperature was thermostatically controlled to 25 °C with the exception of temperature studies where it was increased from 15 °C in 5 °C increments to 50 °C. Buffer solutions were prepared as required from a 50 mM phosphate buffer solution at pH 8 (Table 2) using high purity water

Table 1
Columns prepared for CEC testing

Sample	Column ^a	[SDS] _(aq) (%)	AMPS (% (w/w))	Length to detector (cm)	Pore size (μ m)	Surface area (m ² /g)
1	40:60:30	20	0.3	20	5.3	2.25
2	40:60:20	20	0.3	20	4.9	3.50
3	40:60:40	20	0.3	20	5.8	0.98
4	40:60:40	20	0.6	20	5.8	1.08
5	60:40:40	20	0.3	20	3.3	2.27
6	60:40:20	20	0.3	20	1.7	7.88
7	60:40:40	20	0.3	30	3.3	2.27
8	50:50:50	20	0.3	30	4.5	1.24
9	50:50:50	20	0.3	40	4.5	1.24
10	54:46:34	10	0.6	20	3.3	2.37
11	37:63:29	10	0.6	20	6.6	1.78

^a Column reference, x:y:z, where x:y is the 20% (w/v) SDS_(aq)–1-propanol (w/w) ratio; z the oil concentration (BMA–EDMA, 60:40 (w/w)) in the parent microemulsion.

(Millipore filtered) and acetonitrile. All analytes were dissolved in acetonitrile–buffer (80:20 (v/v); Table 2, Solution 1) to give a concentration of 4 mg/ml. Thiourea was added as an electroosmotic flow (EOF) marker to give a concentration of 1 mg/ml. Columns were conditioned by initial flushing with MeCN–1 mM buffer (80:20) at a pressure of 0.41 MPa for 5 min to observe a flow through the capillary. A voltage of 25 kV was then applied across the capillary until a steady current and a flat baseline were observed. During analysis both vials were pressurised to 0.41 MPa at a run voltage of 20 kV unless otherwise stated. Sample injection was electrokinetic for 3 s at 5 kV.

3. Results and discussion

3.1. Capillary conditioning

After flushing monolithic columns with buffer under pressure, a steady current was achieved within 10 min of the application of an electric field. This current remained steady and constant throughout experiments with a single buffer solution. Upon changing the buffer system, column equilibrium was achieved again within 5 min. In contrast to the monolithic columns, the bead-packed capillaries were unreliable. Initial conditioning was difficult and time consuming. High backpressures require that these bead packed capillaries be conditioned using electroosmosis. Conditioning with different buffer systems frequently required up to and beyond an hour to achieve a steady and stable current. Method development with these columns was time consuming in comparison to the monolithic columns.

3.2. Retention

The retention behaviour of each stationary phase was studied using a test mixture of dipropyl phthalate and diphenyl phthalate. The acetonitrile content of the mobile phase was decreased from 80 to 50% (v/v) at a constant overall ionic strength. In all cases, the retention of the phthalates increased with decreasing acetonitrile concentration and the capacity factors (k) remained stable over several days. Repeat analysis after 3 months storage yielded the same results. In line with reversed-phase HPLC theory, $\ln k$ remains linearly related to percentage acetonitrile content of the mobile phase as shown in Fig. 1. The retention time of the thiourea (added as a flow marker) remained constant as expected, as it has negligible interactions with the stationary phase packing. An example chromatogram can be seen in Fig. 2.

The analytes investigated here are more highly retained on the column packed with ODS particles. The analyte peaks are resolved at higher acetonitrile contents and have much higher retention times (data not shown). This higher retention is due, at least in part, to the much higher surface area obtained with columns packed with porous silica particles ($170 \text{ m}^2/\text{g}$). Typical porous ODS packing have surface areas

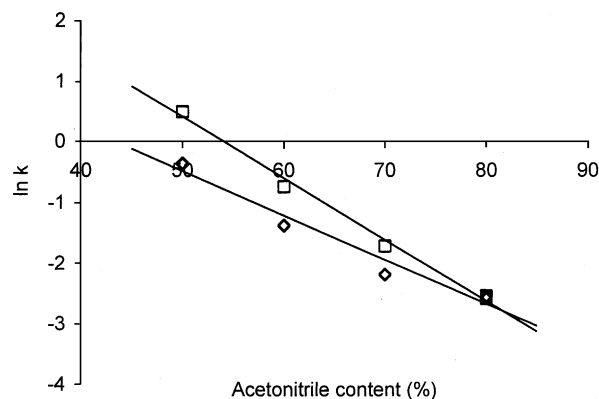


Fig. 1. The effect of acetonitrile content in the mobile phase on $\ln k$ for: (\diamond) dipropyl phthalate and (\square) diphenyl phthalate on a $3.3 \mu\text{m}$ monolithic stationary phase (Table 1, entry 5). Conditions: column: 20 cm monolith length; mobile phase: 1 mM phosphate buffer, pH 8 varying acetonitrile content.

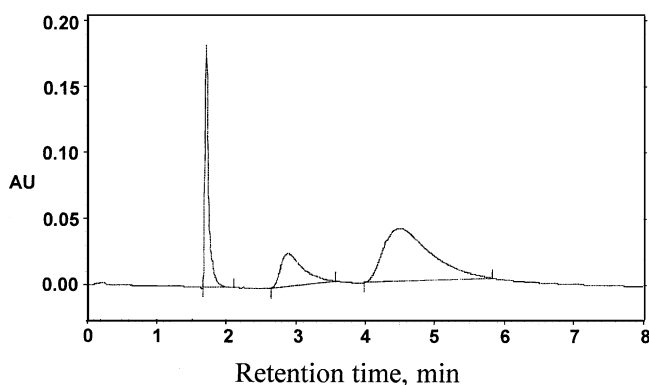


Fig. 2. Electrochromatograms of (in order of elution): thiourea, dipropyl phthalate and diphenyl phthalate in 1 mM total phosphate, pH 8 containing 50% (v/v) acetonitrile. Column: 20 cm monolith length, $3.3 \mu\text{m}$ monolithic packing (Table 1, entry 5).

which are between one and two orders of magnitude greater than those of the porous monolithic materials described here. A higher surface area results in an increased number of binding sites and is evident from the increased gradient in Fig. 3

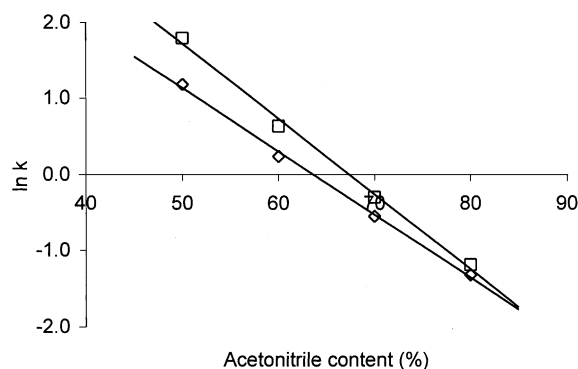


Fig. 3. The effect of acetonitrile content in the mobile phase on $\ln k$ for: (\diamond) dipropyl phthalate and (\square) diphenyl phthalate on $3 \mu\text{m}$ ODS packing. For conditions see Fig. 1.

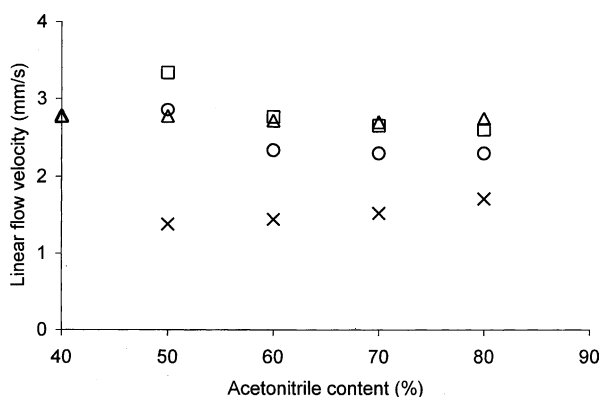


Fig. 4. Effect of acetonitrile content on linear flow velocity for monolithic columns of different pore size ((Δ) 5.8 μm; (□) 5.3 μm; (○) 4.9 μm; (×) 1.7 μm). Conditions: column: 20 cm monolithic length; mobile phase: 1 mM phosphate buffer, pH 8.

compared to Fig. 1. At 50% (v/v) acetonitrile on the ODS columns the capacity factors for dipropyl and diphenyl phthalate are 3.25 and 6.03 respectively. The corresponding retention factors ($\ln k$) for the monolithic columns ranged between 0.3 and 0.8 for dipropyl phthalate, and between 0.8 and 1.7 for diphenyl phthalate.

3.3. Linear flow velocity

In CEC movement of the mobile phase derives from the zeta potential between the stationary and the mobile phases via the electroosmotic mobility.

The von Smoluchowski equation of Eq. (1) shows how the electroosmotic mobility, μ_{eo} , is governed by the zeta potential ζ , the permittivity ϵ_r , the mobile phase viscosity η , the electric field strength E , and the permittivity of a vacuum ϵ_0 :

$$\mu_{eo} = \frac{\epsilon_0 \epsilon_r \zeta E}{\eta} \quad (1)$$

For 20 cm columns with pore sizes of 5.8, 5.3, 4.9, and 1.7 μm, the linear flow velocity obtained from a voltage of 20 kV was measured as a function of the concentration of acetonitrile in the mobile phase (see Fig. 4). Many of the parameters in Eq. (1) will depend upon the acetonitrile concentration of the mobile phase and so the non-linear relationships observed in Fig. 4 are not unexpected. Fig. 4 also shows that the monolith with 1.7 μm pore size gives the lowest linear flow velocity. The inclusion of the additional data given in Fig. 5 demonstrates a linear relationship between pore size and linear flow velocity. It has been shown theoretically by Rice and Whitehead [32] that the linear flow velocity will be independent of diameter, d , only when d is significantly greater than δ . As d approaches δ , double layer overlap will occur resulting in a decrease in linear flow velocity. In the present case, the charged species, 2-acrylamido-2-methyl-1-propane sulfonic acid (AMPS), is added at a constant level (0.3% (w/w), of the monomers),

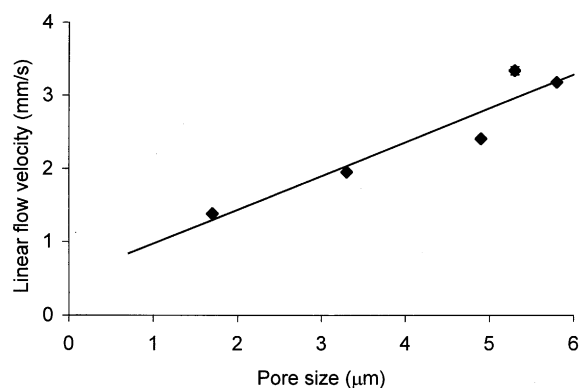


Fig. 5. Effect of pore size on linear flow velocity for monolithic stationary phases prepared using BMA-EDMA (60:40 (w/w)). Conditions: column: 20 cm monolithic length; mobile phase: 1 mM total phosphate buffer, pH 8 containing 50% (v/v) acetonitrile.

therefore it is assumed that the surface coverage is at the same density across all the columns.

Increasing ionic strength results in a reduction in the zeta potential and so the electroosmotic flow. In Fig. 6, the linear flow velocity for the ODS column and two of the monolithic columns is shown as a function of the inverse of the square root of the ionic strength. The linear flow velocity through the monolithic column is greater than through the commercial column. Within the monolithic systems, the surface charge of the packing is easy to alter. When the added AMPS level is doubled there is little change in the resulting linear flow velocity over a range of ionic strengths suggesting a larger increase in AMPS is required to change significantly the effect on the generated electrical double layer.

Compared to the 3 μm ODS packed capillary, the efficiencies of these monolithic columns are low. This could be due to a variety of reasons as yet to be established. Firstly, the surface area of the monolithic columns is significantly lower (by a factor of around 100 times) than that of the ODS beads. This low surface area reduces the number of sites available for partitioning and so the phase is more prone to

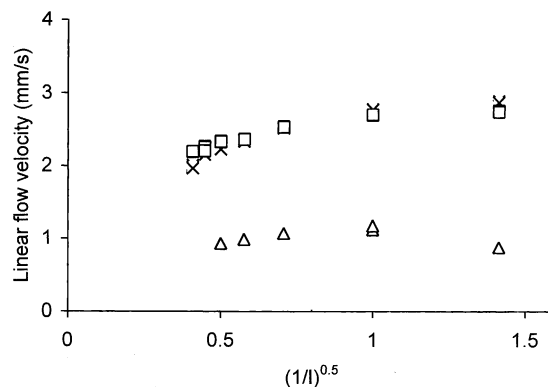


Fig. 6. The effect of buffer ionic strength on linear flow velocity in ODS packed (Δ), and porous monolithic columns. Conditions: column: 20 cm monolithic length; mobile phase: 1 mM total phosphate buffer, pH 8 containing 50% (v/v) acetonitrile (×) 0.3; (□) 0.6% (w/w) AMPS.

Table 3
Column efficiency for monolithic columns of different pore size and lengths monitored for different analytes

		3.3 μm^{a}		4.5 μm^{a}	
		Column length (cm)			
		20	30	30	40
Thiourea	Plates ^b	8093	9424	3533	26,160
	HETP ^c (mm)	0.0247	0.0212	0.057	0.008
	Plates (m) ^d	40,465	31,413	17,666	130,798
Dipropyl phthalate	Plates	1502	1943	2935	5792
	HETP (mm)	0.133	0.103	0.0681	0.0345
	Plates (m)	7510	6477	14,676	28,962
Diphenyl phthalate	Plates	675	899	1707	2773
	HETP (mm)	0.296	0.222	0.117	0.0721
	Plates (m)	3375	2997	8537	13,867

Conditions: column: 20 cm monolith length; mobile phase: 1 mM phosphate buffer, pH 8 containing 60% (v/v) acetonitrile.

^a Pore size: average pore size.

^b Number of theoretical plates per column.

^c Height equivalent to theoretical plate.

^d Number of theoretical plates per metre.

overload. If this effect is significant then increasing the column length will increase the number of theoretical plates. However, in comparing the number of theoretical plates and HETP for two identical columns of different lengths, different values are obtained (Table 3). This suggests that there are other factors affecting the column efficiency and these are possibly dependent on column length. Columns with stationary phases prepared using a BMA–EDMA (60:40 (w/w)) mixture have been studied by other groups. Efficiencies of 32,000 plates/m have been quoted for the separation of basic pharmaceuticals [15] on columns where no porosity data were available. Peters et al. [17–19] reported efficiencies of higher than 120,000 plates/m for the separation of benzene derivatives. These columns have reported pore diameters in the region of 700 nm, therefore the higher efficiencies could be due to increased surface area corresponding to the smaller pore size. However, no surface area measurements are available for these materials.

One of the factors that could affect efficiency is mobile phase and analyte perfusion through the packing. Very relevant effects are eddy diffusion and analyte mass transfer between the mobile, stagnant mobile and stationary phases. If the porous material used for the stationary phase contains dead end pores then the analytes will take a more tortuous path along the column, increasing the time taken for a fraction of the analytes to migrate through the column. Where the right hand side ‘tail’ of the Van Deemter plot has a shallow gradient, a negligible effect from mass transfer mechanisms is implied (Fig. 7). In the case of thiourea for the 4.9 μm column, the plot does not resemble an ‘usual’ Van Deemter plot and H appears to be proportional to the linear flow velocity.

The shape of the plot would seem to suggest that the most significant effect comes from mass transfer mechanisms (the C term in the Van Deemter equation). As the thiourea does

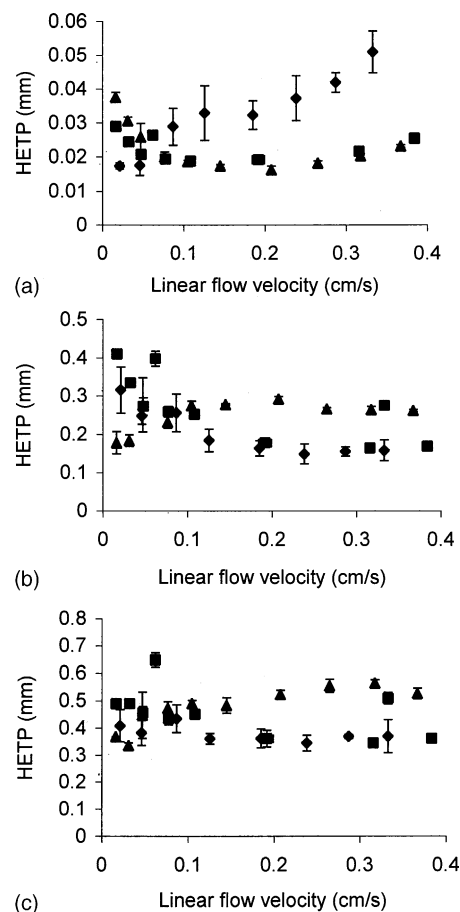


Fig. 7. Van Deemter plots for: (a) thiourea; (b) dipropyl phthalate; and (c) diphenyl phthalate on (◆) 4.9, (■) 5.3 and (▲) 5.8 μm monoliths. Conditions: column: 20 cm monolithic length; mobile phase: 1 mM total phosphate buffer, pH 8 containing 50% (v/v) acetonitrile.

Table 4
Number of theoretical plates for columns of different pore sizes prepared with varying levels of AMPS assessed for different analytes

	3.3 μm^a		5.8 μm^a	
	AMPS (% (w/w))			
	0.3	0.6	0.3	0.6
Thiourea	6186	15,445	7167	7822
Dipropyl phthalate	408	802	599	744
Diphenyl phthalate	215	450	315	349

Conditions: column: 20 cm monolith length; mobile phase: 1 mM phosphate buffer, pH 8 containing 60% (v/v) acetonitrile.

^a Average pore size.

not interact with the stationary phase, this suggests that the mechanism responsible for this decreased efficiency will be transfer between a mobile and stagnant phase. The general case observed here for the monolithic columns is that the linear flow velocity does not appear to have a detrimental effect on efficiency, which will enable the flow rate to be altered to achieve optimum resolution without a major loss of efficiency.

An increased level of AMPS can be seen, in the two cases in Table 4, to increase the column efficiency. An increase in AMPS gives a slight decrease in the linear flow velocity. With a higher level of charged species along the stationary phase surface the electrical double layer produced will be slightly compressed reducing the linear flow velocity. A slightly slower flow rate may be responsible for the increased efficiencies by allowing more analyte–stationary phase interactions during the lifetime of the analyte on the column.

The linear flow velocity was found to be lower through columns with smaller pore sizes. Fig. 8 shows that the efficiency of the thiourea marker is increased with decreasing pore size and vice versa for the phthalate analytes (Fig. 9). The increase in efficiency with pore size for phthalates is coupled with lower surface areas and higher linear velocities.

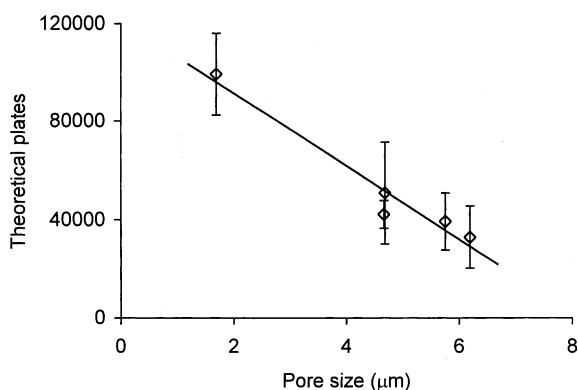


Fig. 8. The effect of pore size on the number of theoretical plates for thiourea. Conditions: column: 20 cm monolithic length; mobile phase: 1 mM total phosphate buffer, pH 8 containing 50% (v/v) acetonitrile.

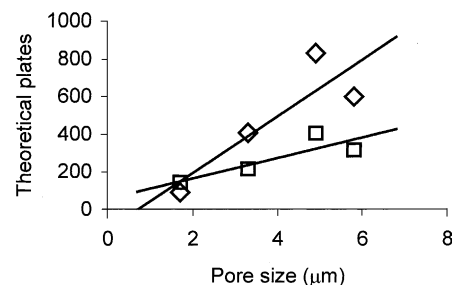


Fig. 9. The effect of pore size on number of theoretical plates for: (\diamond) dipropyl phthalate and (\square) diphenyl phthalate. For conditions see Fig. 8.

3.4. Effect of temperature

A classical description of the adsorption process comes from the Gibbs excess adsorption theory, which considers two similar hypothetical systems with the same volume, temperature, pressure and surface area of the monolith, but which differ in that the first system does not show any adsorption on the surface whereas the second does. K , the equilibrium constant for adsorption of the analyte, is a measure of the interaction energy difference between the eluent and analyte molecules with the monolithic surface. It is proportional to the partition ratio, k , according to Eq. (2), where β is the phase volume ratio.

$$K = \beta \times k \quad (2)$$

The Gibbs standard free energy of the system is related to k by:

$$\Delta G = -RT \ln K \quad (3)$$

and, substituting for K from Eq. (2), it follows that:

$$\Delta G = -RT \ln k - RT \ln \beta \quad (4)$$

Given that:

$$\Delta G = \Delta H - T\Delta S \quad (5)$$

it follows that

$$\ln k + \ln \beta = \frac{-\Delta H}{RT} + \frac{\Delta S}{R} \quad (6)$$

Rearrangement of Eq. (6) enables the enthalpy of transfer of the solute from the mobile to the stationary phase to be determined from the gradient of a logarithmic plot of retention against the inverse temperature as shown in Eq. (7). The entropy of transfer can be determined from the intercept, however, this is difficult due to the non-trivial calculation of the phase ratio in liquid systems.

$$\ln k = \frac{-\Delta H}{RT} + \frac{\Delta S}{R} - \ln \beta \quad (7)$$

Plots of retention against $(1/T)$ for the different monolithic columns and the ODS column were constructed, and the gradient determined and used to calculate ΔH according to Eq. (7). For the different monolithic columns, there is

Table 5
Gradients and calculated standard enthalpies obtained from plots using Eq. (7)

Column reference ^a	Dipropyl phthalate		Diphenyl phthalate	
	Gradient	ΔH (kJ/mol)	Gradient	ΔH (kJ/mol)
40:60:20 (0.3)	881.6	-7.3	304.9	-2.5
40:60:30 (0.3)	728.6	-6.1	802.8	-6.7
40:60:40 (0.3)	622.2	-5.2	800.5	-6.7
40:60:40 (0.6)	1160.9	-9.6	304.7	-2.5
60:40:40 (0.3)	503.4	-4.2	655	-5.4
37:63:29 (0.3)	728.6	-6.1	949.1	-7.9
Hypersil	566.4	-4.7	729	-6.1

^a Concentration of AMPS given in parentheses.

no correlation between enthalpy and pore size at a constant AMPS concentration, however, there is a difference when comparing equivalent columns with different AMPS levels. At 0.6% (w/w) AMPS, the enthalpy for dipropyl phthalate is approximately double that at 0.3% (w/w) (Table 5, entries 3 and 4). It was also noticed that there is significant scatter in the data obtained using the ODS bead-packed column compared to the monolithic columns. Correlation coefficients for the monolithic columns are 0.93–0.99, whereas for the ODS columns they are in the region of 0.63–0.65. Due to the nature of the packing material in the latter, more time is needed for the column to equilibrate to its new conditions.

3.5. Effect on linear flow velocity

From Fig. 10 it can also be seen that the increase in linear flow velocity is directly proportional to temperature. This is due to an inverse relationship between temperature and mobile phase viscosity. An increase in temperature also results in an increase in current generated. As the capillary is analogous to a cylindrical conductor, resistive (Joule) heat is produced on the application of a voltage when a current flows. The quantity of heat generated per volume of electrolyte, Q , can be calculated using Eq. (8), where λ is the molar con-

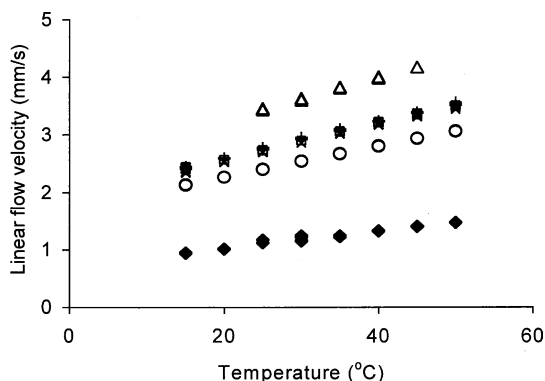


Fig. 10. The effect of temperature on linear flow velocity in monolithic columns (+, ○, □, ×) 1–4, (△) 11 and (◆) an ODS packed column (see Table 1 for compositions of monoliths). Conditions: column: 20 cm monolithic 3 length; mobile phase: 1 mM total phosphate buffer, pH 8 containing 50% (v/v) acetonitrile.

ductivity, c the concentration of electrolyte and ϵ the total porosity. The heat is dissipated by conduction through the capillary wall and surrounding air (or liquid in temperature controlled systems). The gradients of the plots in Fig. 10 are all similar suggesting that the heat produced in each column is easily dissipated.

$$Q = E^2 \lambda c \epsilon \quad (8)$$

4. Conclusions

The initial columns investigated show potential as stationary phases for capillary electrochromatography, although further column optimisation is required to improve efficiency. Monolithic columns show several advantages over traditional packed capillaries: their ‘hands on’ preparation time is short and many capillaries can be prepared simultaneously from one batch of microemulsion at one time (potentially increasing reproducibility); conditioning of the columns prior to use is quick and reliable allowing rapid method development. The columns themselves exhibit characteristics necessary for use as separation media. An alteration of the mobile phase system allows analyte capacity to be altered enabling method development with different analytes. Large pore diameters allow the use of low ionic strengths without the concerns of electrical double layer overlap experienced using columns packed with ODS beads. Further development of these packing materials is required to gain an understanding of the effects of channel size and distribution on this.

Column inhomogeneity or instability cannot be ruled out as possible sources of poor column efficiency. However, performance was found to be reproducible and stable over a 3-month period. In addition, extrusion of the packing material from the capillary did not occur until backpressure exceeded 20 MPa, suggesting that the monolith adhered well to the capillary wall. Furthermore, inspection of columns with an optical microscope prior to use in CEC did not reveal any inhomogeneity. Future work will involve the use of a siloxane monomer in order to bond the monolith chemically to the capillary, to investigate this point further.

Acknowledgements

The EPSRC and Astra Zeneca are thanked for funding this research.

References

- [1] K.D. Altria, J. Chromatogr. A 856 (1999) 443.
- [2] M.M. Dittmann, G.P. Rozing, J. Chromatogr. A 744 (1996) 63.
- [3] C. Fujimoto, Trends Anal. Chem. 18 (1999) 291.
- [4] F.E. Regnier, J. High Resolut. Chromatogr. 23 (2000) 19.

- [5] R. Asiaie, X. Huang, D. Farnan, C. Horvath, J. Chromatogr. A 806 (1998) 251.
- [6] C. Fujimoto, Y. Fujise, E. Matsuzawa, Anal. Chem. 68 (1996) 2753.
- [7] C. Fujimoto, J. High Resolut. Chromatogr. 23 (2000) 89.
- [8] N. Tanaka, H. Nagayama, H. Kobayashi, T. Ikegami, K. Hosoya, N. Ishizuka, H. Minakuchi, K. Nakanishi, K. Cabrera, D. Lubda, J. High Resolut. Chromatogr. 23 (2000) 111.
- [9] Q.L. Tang, M.L. Lee, J. High Resolut. Chromatogr. 23 (2000) 73.
- [10] T.M. Zimina, R.M. Smith, P. Myers, J. Chromatogr. A 758 (1997) 191.
- [11] M. Kato, M.T. Dulay, B. Bennett, J.R. Chen, R.N. Zare, Electrophoresis 21 (2000) 3145.
- [12] S. Hjertén, Ind. Eng. Chem. Res. 38 (1999) 1205.
- [13] A. Maruska, C. Ericson, A. Vegvari, S. Hjertén, J. Chromatogr. A 837 (1999) 25.
- [14] A. Palm, M.V. Novotny, Anal. Chem. 69 (1997) 4499.
- [15] D. Hindocha, N.W. Smith, Chromatographia 55 (2002) 203.
- [16] J.L. Liao, N. Chen, C. Ericson, S. Hjertén, Anal. Chem. 68 (1996) 3468.
- [17] E.C. Peters, M. Petro, F. Svec, J.M.J. Fréchet, Anal. Chem. 69 (1997) 3646.
- [18] E.C. Peters, M. Petro, F. Svec, J.M.J. Fréchet, Anal. Chem. 70 (1998) 2288.
- [19] E.C. Peters, M. Petro, F. Svec, J.M.J. Fréchet, Anal. Chem. 70 (1998) 2296.
- [20] I. Gusev, X. Huang, C. Horváth, J. Chromatogr. A 855 (1999) 273.
- [21] X.A. Huang, S. Zhang, G.A. Schultz, J. Henion, Anal. Chem. 74 (2002) 2336.
- [22] J. Haginaka, J. Chromatogr. A 875 (2000) 235.
- [23] M. Lammerhofer, W. Lindner, J. Chromatogr. A 829 (1998) 115.
- [24] M. Lammerhofer, F. Svec, J.M.J. Fréchet, W. Lindner, Trends Anal. Chem. 19 (2000) 676.
- [25] M. Lammerhofer, F. Svec, J.M.J. Fréchet, W. Lindner, J. Microcol. Sep. 12 (2000) 597.
- [26] T. Takeuchi, J. Matsui, J. High Resolut. Chromatogr. 23 (2000) 44.
- [27] M.G. Schmid, N. Grobuschek, C. Tuscher, G. Gubitz, A. Vegvari, E. Machtejevas, A. Maruska, S. Hjertén, Electrophoresis 21 (2000) 3141.
- [28] D. Josic, A. Buchacher, A. Jungbauer, J. Chromatogr. B 752 (2001) 191.
- [29] L. Kvasničková, Z. Glatz, H. Štirbová, V. Kahle, J. Slanina, P. Musil, J. Chromatogr. A 916 (2001) 265.
- [30] K.J. Flook, Ph.D. Thesis, University of Durham, 2003.
- [31] N.R. Cameron, K.J. Flook, S.A.C. Wren, Chromatographia 57 (2003) 203.
- [32] C.L. Rice, R. Whitehead, J. Phys. Chem. 69 (1965) 4017.